Assessment of active fire detection in Serra da Canastra National Park using MODIS and VIIRS sensors

Guilherme S. Pinto [1*], Henrique Bernini [1], Cassiano G. Messias [1], Otávio A. S. Silva [1], Paulo W. Cunha [1], Paulo S. Victorino [1], Fabiano Morelli [1]
[1] National Institute for Space Research (INPE) - Brazil
[*] guilherme.pinto@inpe.br

Keywords: Active fire; Wildfire; National Park; Remote sensing; Burned area.

Abstract

The geographic data utilization for the occurrence of wildfires and forest fires for monitoring fire usage in vegetation has become increasingly important for generating information that aids in decision-making and policy development regarding climate change and its impacts. This study aims to validate the active fire data processed by INPE’s *Queimadas* Program at *Serra da Canastra* National Park during the first semester of 2023. This period is characterized by lower intensity of fire thermal radiation due to meteorological and climatic factors such as lightning, precipitation, and temperature. We compared active fire data from the MODIS and VIIRS sensors with 220 fire scars mapped by the Sentinel-2 satellite. Additionally, we analyzed the distribution of active fire data across different classifications of fire scar size. The validation rate was 99.4% for VIIRS and 95% for MODIS, with few commission errors (false positives). However, omissions (false negatives) were observed in detecting scars smaller than 1 km², related to both sensor characteristics and fire behavior. The results were satisfactory, indicating that future studies can further refine this research.

1. Introduction

Ecosystems in different Brazilian biomes vary in their response and vulnerability to fire. Ecosystems characterized by the dominance of grasses, such as those located in the *Cerrado* biome, have coevolved with fire, and their plants exhibit various adaptations and synergies with it; the biome is considered as fire-dependent, from an ecological perspective. Anthropic fires, however, have reached record levels in the past 20 years (PIVELLO, 2021). Most fires occur in the transition zone between the Cerrado and Amazon biomes, in the region known as the arc of deforestation. Between 2001 and 2018, 62.2% of the fire scars occurring in Brazilian biomes were in the *Cerrado* (ALVES & ALVARADO, 2019).

The growing concern about climate change and global warming underscores the need for responses to increasingly intense environmental challenges such as wildfires, which result in economic losses, exacerbate health problems, and negatively impact to biodiversity (PIVELLO et al., 2021; GRAN & RUNKL, 2021). Additionally, these fires contribute to the increase of carbon emissions into the atmosphere (GATTI et al., 2023).

Aiming to contribute to more agile and strategic decision-making, the National Institute for Space Research (*Instituto Nacional de Pesquisa Espaciais*, INPE) has been improving its fire and deforestation monitoring programs since the 1980s. The active fire data produced by INPE uses orbital images from 11 different satellites, which allow the identification of areas where fire has been present in vegetation. This product has been widely used for the fire management, particularly in remote areas, through early identification of wildfire occurrences, enabling rapid response to these events (SETZER et al., 2021). It is also used for monitoring on the productive areas to prevent fires from spreading and causing material damage.

The active fires identification through algorithms developed for the MODIS and VIIRS sensors is based on the thermal anomalies and spectral reflectance across multiple bands. Both sensors utilize brightness temperature and reflectance data to detect fire pixels, distinguishing them from other heat sources through threshold and spatial tests, covering bands ranging from red to thermal infrared (SCHROEDER & GIGLIO, 2018; GIGLIO et al., 2021). Consequently, these high-temperature areas on the Earth's surface are detected and converted into geographically referenced active fire points.

On the other hand, fire in vegetation leaves a signature on orbital images related to residual ashes and charcoal, which are used to map burn scars by observing changes in the spectral characteristics of the vegetation. The deposition of charcoal temporarily darkens the surface, while changes in vegetation structure are more enduring. Consequently, the burned areas detection is possible due to the difference in spectral behavior between burned and unburned areas, although cloud coverage and shadows complicate the mapping process (PEREIRA et al., 1999). The intensity of the fire, influenced by atmospheric conditions and the characteristics of the burned material, also affects the signals in the images (LIBONATI et al., 2011).

This study analyzed the spatial and temporal distribution of active fire data detected by the MODIS (onboard the AQUA and TERRA satellites) and VIIRS (onboard the NOAA-20 and Suomi NPP satellites) sensors in the *Serra da Canastra* National Park (SCNP), located in *Minas Gerais* (Figure 1), during the first semester of 2023. The analysis was conducted across different classes and sizes of burn scars mapped using Sentinel-2 images. The study area is located within the *Cerrado* biome, and the period analyzed is characterized by less intense fires compared to the second semester of the year as the dry season progresses.

The SCNP has extensive areas with a high risk of fire spread. Large areas located on the tops of plateaus are burned annually — areas of higher relief with convex slopes, primarily composed of open fields, which are highly affected by wind and have low densities of circulation and drainage (MESSIAS & FERREIRA, 2019). Therefore, the SCNP is an excellent area for studies related to fire in the *Cerrado*.

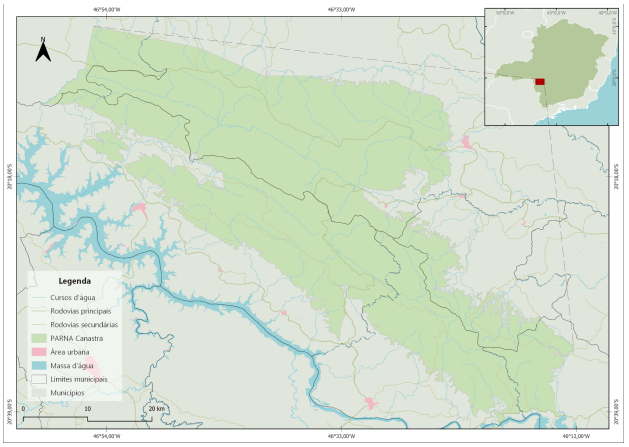

Figure 1. Location of the study area

2. Materials and Methods

The burned areas were mapped using images from the Sentinel 2 satellites (A and B) (ESA, 2023), with a temporal resolution of 5 days and a spatial resolution of 20 meters for bands B11 and B12. The mapping was conducted using 39 images with low cloud coverage in the study area between January and June 2023. The Normalized Burn Ratio SWIR (NBR SWIR) index (Equation 1) was calculated both before and after the fire events (Liu et al., 2020). Later, the differences between the images (Equation 2) were utilized to highlight the changes and extract the burned area scars (figure 2).

$$NBR\ SWIR = \frac{(S1 - S2 - 0.02)}{(S1 + S2 + 0.1)} \quad (1)$$

Where S1 and S2 are shortwave infrared bands, specifically SWIR1 (B11) and SWIR2 (B12).

$$\Delta NBR\ SWIR = \frac{NBR\ SWIR_{pre-fire} - NBR\ SWIR_{post-fire}}{(ABS)\ NBR\ SWIR_{pre-fire}} \quad (2)$$

Where ABS indicates the absolute value, avoiding division by negative numbers.

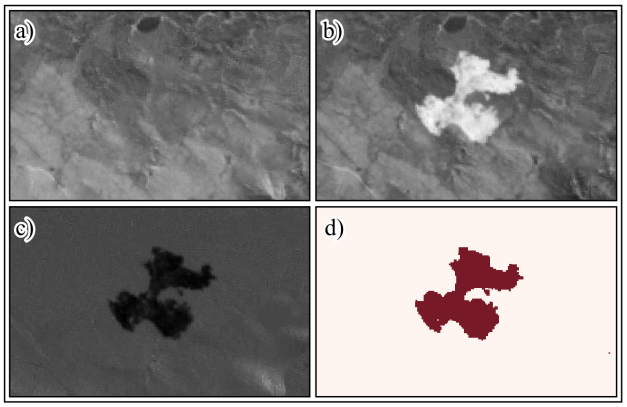

Figure 2. Example of the burned area mapping process: a) NBR SWIR before the fire occurrence; b) NBR SWIR after the fire occurrence; c) differences between the images; d) burn scar.

The active fire data were obtained from the *BDQueimadas* platform (INPE, 2023). Each detected active fire point corresponds to the centroid of the pixel that registered the infrared radiation from the fire at the moment of the sensor's passage. To represent the specific area of the Earth's surface captured by the sensor, rectangular buffers were generated corresponding to each pixel of active fire detection. These buffers have dimensions relating to the pixel size along the scan (along-scan pixel) and the pixel size along the track (along-track pixel) of the sensor that detected the respective active fire. The size of these pixels varies according to the location of the detected active fire relative to nadir, based on the distance along the scan. (NASA Worldview, 2024). This variation is known as the Bowtie effect.

The bowtie effect is a common characteristic in wide-scan sensors like MODIS and VIIRS, resulting in pixel distortion on the borders of the imaging track due to the distance of the IFOV (Instantaneous Field of View) of NADIR (Figure 3). The sensor scan angle affects the spatial resolution of collected data and it impacts the detection of active fire. According to Ruddorf et al. (2007), the border pixels can be up to five times larger and two times wider than the pixels in the center of the track on the MODIS sensor. In the opposite way, the VIIRS sensor was designed to minimize the Bowtie effect, with the maximum pixel size at the scan edge being approximately twice the nadir pixel size (Wolfe et al., 2013).

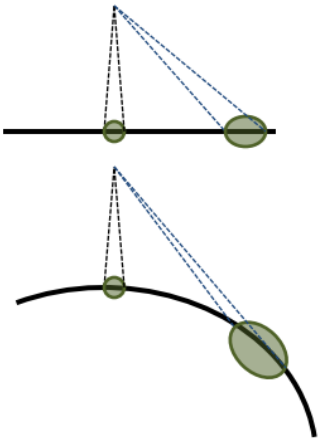

Figure 3. Simplified representation of the Bowtie effect (NASA, Earthdata, 2024).

This way, it is possible to identify the dimension of the active fire distortion, considering its distance to the burned area, allowing a better recognition of commission error, where the data of active fire does not intersect its corresponding burned area. Omission (false negative) on the other hand occurs when there is no occurrence of active fire on the burned area.

The mapped burn scars were categorized into four size intervals representing the nominal pixel size of medium and low spatial resolution sensors: 1) 0 - 0.06 km²; 2) 0.06 - 0.25 km²; 3) 0.25 - 1 km²; and 4) 1 - 16 km².

The detected active fire data were analyzed across different extents of burned areas. Each mapped scar is associated with the active fire detection during the same period of occurrence, i.e., between the dates immediately before and after the occurrence of the represented burned area.

3. Results and Discussion

3.1 Detection and classification of burned Areas

The mapping methodology employed allowed the detection of 153.58 km² of burned areas during the analyzed period,

distributed across 220 polygons of burn scars. As represented in Table 1, the most frequent scars (162 scars) are those with dimensions smaller than 0.25 km², representing nearly three-quarters of the total scars detected.

Interval classes (km²)	Number of scars	(%)	Total area (km²)	(%)
0 - 0.06	102	46.4	2.20	1.4
0.06 - 0.25	60	27.3	7.36	4.8
0.25 - 1	32	14.5	16.57	10.8
1 - 16	26	11.8	127.44	83.0
Total	220	100	153.58	100

Table 1. Size interval classes for burn scars by number of scars and accumulated burned area.

However, the combined burned area for this same size class represents only 6.2% of the total mapped area, indicating a high occurrence of small-scale wildfires. Burned area scars with larger dimensions (> 1 km²), although less frequent (26 scars), represent 83% of the total mapped area.

The shape of burn scars is closely related to the characteristics of the regions affected by the fire, including terrain, vegetation, and the prevailing climatic conditions at the time of the event. In the SCNP, the predominance of grassland vegetation, combined with a high accumulation of vegetative fuel load during the dry season, makes these areas particularly susceptible to fire. The low population density in elevated regions, such as the "*Chapadões*," contributes to reduced human intervention in fire prevention and fighting. Additionally, these areas are frequently exposed to stronger winds due to their altitude, which intensifies fire propagation. The absence of natural barriers, such as watercourses and roads, further facilitates the spread of flames compared to lower areas. The mapping conducted in this study corroborates the analyzes by Messias and Ferreira (2019), which highlight the vulnerability of elevated areas of the SCNP to the occurrence of wildfires.

3.2 Occurrence of active fires in burned areas

The MODIS sensor detected a total of 60 active fires during the analyzed period. Of these, 57 were validated as active fires, resulting in a validation rate of 95%. The remaining 3 active fires, which were not validated, had detection pixel borders at distances ranging from 170 to 480 meters from the mapped burn scars. This distance corresponds to less than the nominal pixel width of 1 km for the MODIS sensor, suggesting that these cases could be considered false positives.

The Figure 4 illustrates a buffer representation of an active fire pixel detected on February 8 and validated with the burned area mapping between January 29 and February 23. The rectangle with the continuous line represents the nominal pixel of the MODIS sensor with dimensions of 1 km x 1 km, while the rectangle with dashed lines represents a pixel whose dimensions vary according to the along-scan and along-track pixels, reflecting the distance from the nadir angle and resulting in some distortion. Therefore, it can be observed that the detection pixel of the active fire, represented by the dashed buffer, partially intersects with the burned area. This is an example of an active fire detected that initially could be considered a false positive but was validated.

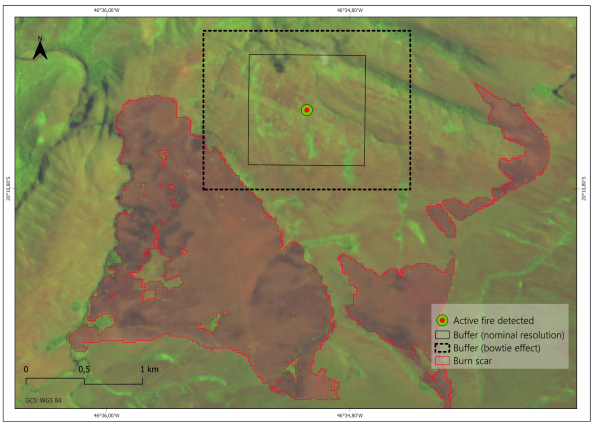

Figure 4. Representation of the active fire detection pixel through the creation of a buffer for validation.

The Figure 5 illustrates the detection of a false positive. The active fire was detected on June 5, and its respective burn scar was mapped between May 23 and June 8.

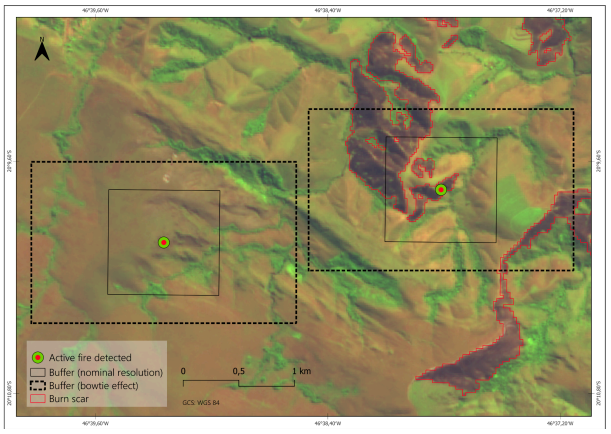

Figure 5. Identification of a false-positive of active fire (left) through the creation of a buffer for validation.

It can be observed that the detection on the left occurred over an area that had burned weeks earlier, indicating possible "contamination" by the influence of a neighboring pixel on the right, which was validated with a burn scar.

The VIIRS sensor detected 462 active fires. Of these, 459 (~99%) were validated, while 3 active fires did not intersect the burned area within the corresponding time span. The distance from the border of these burned pixels ranged from 20 to 145 meters from the burn scar, which corresponds to an error smaller than the nominal pixel width of 375 meters. The potential false alarms identified may be associated with the contamination of neighboring pixels, which can occur due to the high intensity of the fire increasing the brightness of the active fire pixel or due to smoke plumes containing particles sufficiently hot to trigger the pixel.

The burn scar mapping indicated the absence of active fire data for intersection during the respective period, characterizing an omission error in this product, as illustrated in the Figure 6. The red areas represent burn scars intersected by active fires detected within the same period, indicating a precise correspondence between the detection data and the actual state of the vegetation. Conversely, the blue areas represent false negatives, where active fires were not detected despite the presence of burn scars.

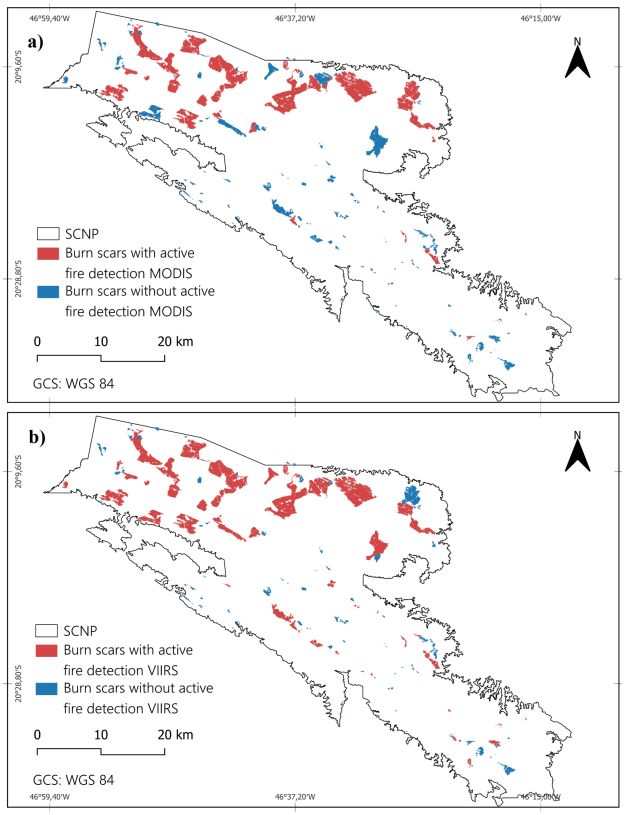

Figure 6. Burned area scars with and without the active fire occurrence detected by sensors a) MODIS and b) VIIRS.

The MODIS sensor omitted 184 burn scars, totaling 45.13 km², which represents 29.4% of the burned areas identified as false negatives, as shown in Table 2. In other words, these were fire events that were not detected by the sensor.

	Validated		Not validated	
Interval classes (km²)	Number of scars	Total area (km²)	Number of scars	Total area (km²)
0 - 0.06	5	0.11	97	2.09
0.06 - 0.25	4	0.50	56	6.86
0.25 - 1	9	5.10	23	11.47
1 - 16	18	102.72	8	24.71
Total	36	108.44	184	45.13

Table 2. Number of burned area scars and their corresponding validated and non-validated areas by the MODIS sensor.

It is observed that half of the sensor’s detections occurred in scars larger than 1 km², suggesting that MODIS is more efficient in identifying large-scale burned areas. This pattern indicates that the sensor may have difficulties detecting smaller scars, possibly due to its spatial resolution, which limits the ability to identify fire events with precision in smaller areas.

The VIIRS sensor demonstrated superior performance in detecting burn scars compared to MODIS. Although it omitted 149 scars, totaling 22.11 km², VIIRS excelled in its capacity to identify a larger number of smaller scars, with sizes less than 100 hectares. The omission accounted for only 14.4% of the total burned area for the analyzed period. This performance is highlighted in Table 3, which shows how VIIRS detects smaller-scale burned areas with greater precision, when compared to MODIS.

	Validated		Not validated	
Interval classes (km²)	Number of scars	Total area (km²)	Number of scars	Total area (km²)
0 - 0.06	17	0.46	85	1.74
0.06 - 0.25	15	1.89	45	5.47
0.25 - 1	15	8.83	17	7.74
1 - 16	24	120.28	2	7.15
Total	71	131.47	149	22.11

Table 3. Number of burned area scars and their corresponding validated and non-validated area by the VIIRS sensor.

It is important to note that the occurrence of dense cloud coverage over the active fire during the satellite pass, or the presence of fire fronts with low extent or intensity, are examples of factors that can contribute to the occurrence of false negatives. Some burn scars may have been generated in a short time span, precisely during a period when the area was not imaged by these sensors. This can occur due to the rapid fire propagation through certain vegetation types of the *Cerrado* biome, especially grassland formations, also influenced by terrain, wind speed, and temperature.

In the literature, similar results have been observed when validating INPE’s *Queimadas* Program products for active fire detection using burned area data. Studies by Jesus et al. (2011), Gontijo et al. (2011), and Pereira et al. (2012) confirm these results, demonstrating that the validation of active fire detection products often reveals common patterns and limitations. These studies highlight that, although fire detection products provide a valuable tool for wildfire monitoring, the precision in identifying burned areas can vary depending on the resolution and validation method used. Therefore, the results presented in this study align with the existing literature, underscoring the importance of considering specific sensor characteristics and validation methodologies to enhance accuracy in fire detection and mapping.

4. Conclusion

The results of this study corroborate similar conclusions in the literature regarding active fire detection through satellite sensors. The active fire data detected by MODIS and VIIRS, analyzed outside a critical period of wildfires, demonstrate the ability to accurately detect fire occurrences when their intensity is considered lower, although with differences in performance.

The VIIRS sensor demonstrated significantly better performance in spatial sampling compared to MODIS. Its ability to minimize pixel size distortion with the scan angle resulted in more refined performance in mapping active fires in vegetation. By reducing pixel distortion, VIIRS allows for the identification of active fires with greater precision, even in smaller and less intense fire fronts.

VIIRS was able to detect active fires corresponding to a larger number of burn scars with dimensions smaller than 1 km². In contrast, MODIS presented limitations in detecting active fires that correspond to smaller areas due to its spatial resolution and the pixel distortion effect, requiring the active fire to be larger or more intense to be reliably detected.

Sensors with higher spatial resolution, like VIIRS, have a better capacity for detecting smaller fires compared to sensors with moderate resolution, like MODIS. The reason is that smaller pixels reduce the probability of containing a mix of burned and unburned areas, resulting in a clearer thermal signature for fires.

Although both sensors presented a high rate of validation, with VIIRS reaching 99.4% and MODIS 95%, the omission in active fire detection corresponding to smaller scars for both sensors highlights their limitations. Factors such as cloud coverage, the intensity and extent of the fire, and the timing of satellite imaging over affected areas directly impact data detection and precision.

In the *Serra da Canastra* National Park, the detection of small burned areas (with sizes less than 1 km²) is limited by the technical constraints of both sensors. However, the results of this research demonstrate that active fire data are excellent indicators for monitoring vegetation fires, enabling quick and effective wildfire management actions as well as scientific applications.

The research emphasizes the importance of combining different sensors and methodologies for more robust and effective wildfire monitoring. Future studies that include field analysis and consider meteorological data and fire behavior can further enhance data accuracy and improve fire management strategies.

Acknowledgments

Thanks to the National Council of Technological and Scientific Development - CNPq project number 422354/2023-6 (MONITORAMENTO E AVISOS DE MUDANÇAS DE COBERTURA DA TERRA NOS BIOMAS BRASILEIROS – CAPACITAÇÃO E SEMIAUTOMATIZAÇÃO DO PROGRAMA BIOMASBR) and 382775/2022-8, supported by the National Institute for Space Research (INPE). I thank the National Council for Scientific and Technological Development for the research fellowship (Grants nº 384915/2023-0 and 382775/2022-8, respectively).

References

Alves, D. B., Alvarado, S. T., 2019. Variação espaço-temporal da ocorrência de fogo nos biomas brasileiros com base na análise de produtos de sensoriamento remoto. *Geografia*, 44:2, 231-345. DOI: 10.5016/geografia.v44i2.15119.

ESA. European Space Agency. Copernicus, 2023. URL http://scihub.copernicus.eu/dhus/#/home (02 Jun. 2023).

Gatti, L.V., Cunha, C.L., Marani, L. et al., 2023. Increased Amazon carbon emissions mainly from decline in law enforcement. *Nature*, 621, 318–323. doi.org/10.1038/s41586-023-06390-0.

Giglio, L., Schroeder, W., Justice, C. O., 2016. The collection 6 MODIS active fire detection algorithm and fire products. *Remote Sensing of Environment*, 178:31-41. 2016. doi.org/10.1016/j.rse.2016.02.054.

Gontijo, G. A. B., Pereira, A. A., Oliveira, E. D. S., Acerbi Jr., F. W., 2011. Detecção de queimadas e validação de focos de calor utilizando produtos de Sensoriamento Remoto. Ann. *XV Simpósio Brasileiro de Sensoriamento Remoto: INPE*, 7966-7973. DOI:10.13140/2.1.3401.4726.

Grant, E., Runkle, J. D., 2022. Long-term health effects of wildfire exposure: A scoping review. *The Journal of Climate Change and Health*, Volume 6, 100-110, doi.org/10.1016/j.joclim.2021.100110.

INPE, Instituto Nacional de Pesquisas Espaciais, 2023. Banco de Dados de queimadas. URL http://inpe.br/queimadas/bdqueimadas (10 Jul. 2023).

Jesus, S. C., Setzer, A. W., Morelli, F., 2011. Validação de focos de queimadas no Cerrado em imagens TM/Landsat-5. Ann. *XV Simpósio Brasileiro de Sensoriamento Remoto: INPE*, 8051-8058. URL http://dsr.inpe.br/sbsr2011/files/ p0899.pdf (25 Mar. 2024).

Libonati, R., Pereira, A. A., Santos, F. L. M., Rodrigues, J. A., Santa Rosa, A., Melchiori, A. E., Morelli, F., Setzer, A. W., 2011. Sensoriamento remoto de áreas queimadas no Brasil: progresso e incertezas, desafios e perspectivas futuras. In: Setzer A. W., Ferreira, N. J. *Queimadas e incêndios florestais: mediante monitoramento orbital*. Oficina de textos: São Paulo.

Liu, S., Zheng, Y., Dalponte, M., Tong, X., 2020. A novel fire index-based burned area change detection approach using Landsat-8 OLI data, *European Journal of Remote Sensing*, 53:1, 104-112. doi.org/10.1080/22797254.2020.1738900.

Messias, C. G., Ferreira, M. C., 2019. Modelo geoespacial para a identificação de áreas com perigo de propagação de queimadas no Parque Nacional da Serra da Canastra. *Revista do Departamento de Geografia*, v. 38, 154-168.

NASA Earthdata., 2024. VIIRS I-Band 375 m Active Fire Data. NASA Earthdata. URL http://earthdata.nasa.gov/learn/find-data/near-real-time/firms/viirs-i-band-375-m-active-fire-data (05 April 2024).

NASA Worldview., 2024. NASA Worldview Earthdata. NASA. URL http://worldview.earthdata.nasa.gov/ (05 April 2024).

Pereira, A. A., Pereira, J. A. A., Morelli, F., Barros, D. A., Acerbi Jr., F. W., & Scolforo, J. R. S., 2012. Validação de focos de calor utilizados no monitoramento orbital de queimadas por meio de imagens TM. *CERNE*, 18(2), 335–343. doi.org/10.1590/S0104-77602012000200019.

Pereira, J. M. C., Sá, A. C. L., Sousa, A. M. O., Silva, J. M. N., Santos, T. N., Carreiras, J. M. B., 1999. Spectral characterisation and discrimination of burnt areas. In: Chuvieco, E. (ed.). *Remote Sensing of large wildfires*. Springer, Berlin Heidelberg. 123-138. doi.org/10.1007/978-3-642-60164-4_7.

Pivello, V. R., Vieira, I., Christianini, A. V. et al., 2021. Understanding Brazil’s catastrophic fires: Causes, consequences and policy needed to prevent future tragedies. *Perspectives in Ecology and Conservation*, Volume 19, Issue 3, 233-255, ISSN 2530-0644, doi.org/10.1016/j.pecon.2021.06.005.

Rudorff, B. F. T., Shimabukuro, Y. E., Ceballos, J. C. (orgs.)., 2007. *O sensor MODIS e suas aplicações ambientais no Brasil*. São José dos Campos: Editora Parêntese, 425 p.

Schroeder, W., Giglio, L., 2018. NASA VIIRS Land Science Investigator Processing System (SIPS) Visible Infrared Imaging Radiometer Suite (VIIRS) 375 m & 750 m Active Fire Products Product User’s Guide Version 1.4. NASA. URL http://lpdaac.usgs.gov/documents/427/VNP14_User_Guide_V1.pdf (02 July 2023).

Setzer, A. W., Victorino, P. S. S., Bottino, M. J., 2021. Detecção de queimadas por satélites geoestacionários e seu uso no Programa Queimadas do INPE. In: Setzer A. W., Ferreira, N. J. *Queimadas e incêndios florestais: mediante monitoramento orbital*. São Paulo.

Wolfe, R. E., Lin, G., Nishihama, M., Tewari, K. P., Tilton, J. C., & Isaacman, A.R., 2013. Suomi NPP VIIRS prelaunch and on-orbit geometric calibration and characterization. *Journal of Geophysical Research: Atmospheres*, 118. 10.1002/ jgrd.50873.